ACS Synthetic Biology
Cite This: ACS Synth. Biol. 2019, 8, 1913−1920
Research Article
pubs.acs.org/synthbio

An Adaptive Synthetic Cell Based on Mechanosensing, Biosensing, and Inducible Gene Circuits

Jonathan Garamella,[†,#] Sagardip Majumder,[‡,#] Allen P. Liu,[*,‡,§,∥,⊥] and Vincent Noireaux[*,†]

[†]Department of Physics and Astronomy, University of Minnesota, Minneapolis, Minnesota 55455, United States
[‡]Department of Mechanical Engineering, [§]Department of Biomedical Engineering, [∥]Cellular and Molecular Biology Program, [⊥]Biophysics Program, University of Michigan, Ann Arbor, Michigan 48109, United States

Supporting Information

ABSTRACT: The bottom-up assembly of synthetic cell systems capable of recapitulating biological functions has become a means to understand living matter by construction. The integration of biomolecular components into active, cell-sized, genetically programmed compartments remains, however, a major bottleneck for building synthetic cells. A primary feature of real cells is their ability to actively interact with their surroundings, particularly in stressed conditions. Here, we construct a synthetic cell equipped with an inducible genetic circuit that responds to changes in osmotic pressure through the mechanosensitive channel MscL. Liposomes loaded with an *E. coli* cell-free transcription−translation (TXTL) system are induced with IPTG when exposed to hypo-osmotic solution, resulting in the expression of a bacterial cytoskeletal protein MreB. MreB associates with the membrane to generate a cortex-like structure. Our work provides the first example of molecular integration that couples mechanosensitivity, gene expression, and self-assembly at the inner membrane of synthetic cells.

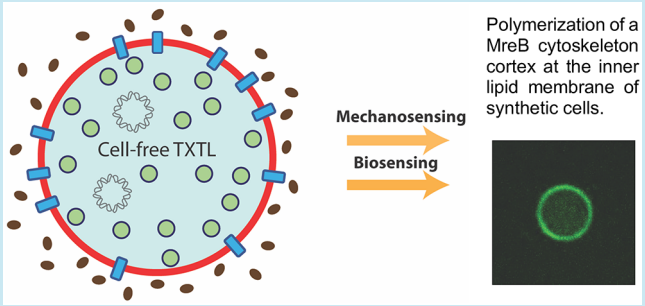

KEYWORDS: *synthetic cell, MscL, cell-free transcription−translation (TXTL), gene circuits, biosensing*

Building genetically encoded microscopic compartments capable of mimicking functions of real living cells has become a conceivable, yet challenging, goal of synthetic biology.[1−3] While the top-down approach consists of stripping down a living cell to a minimum set of components,[4] the bottom-up approach attempts to build a functioning cell by assembling components from scratch.[5−9] Bottom-up synthetic cells are micron-sized compartments, programmed with elementary gene networks or purified proteins, that recapitulate specific cellular functions in isolation. In such settings, fundamental questions can be addressed by quantitative molecular construction. Apart from being at the cutting edge of biological engineering, synthetic biology, and biophysics, bottom-up synthetic cells are also particularly interesting for developing applications geared toward biotechnologies and medicine.[10] Integrating components into truly active cell analogues remains, however, a major bottleneck in synthetic cell research.[2]

A major approach to bottom-up synthetic cells consists of encapsulating a cell-free expression system into cell-sized liposomes.[11−15] Such systems can be programmed with gene networks to isolate and engineer single biological functions.[8,16,17] Transcription−translation (TXTL) has become a versatile and effective tool for prototyping biomolecular systems over a broad range of physical scales, from gene circuits to synthetic cells.[18] The major advantage of TXTL is to dramatically reduce the design-build-test cycle from days or weeks, for *in vivo* experiments, to hours. The all *E. coli* TXTL used in this work is highly programmable, having access to the full set of *E. coli* sigma factors, allowing the construction of complex gene circuits from both plasmid and linear DNA.[19] Our goal is to demonstrate that TXTL-based synthetic cells can cooperatively link, like in real living cells, DNA information, metabolism, and self-assembly. Herein, we describe results that build upon our prior work involving the *E. coli* mechanosensitive channel of large conductance (MscL) and a calcium sensing recombinant protein, G-GECO.[17] We advance beyond biosensing by developing a synthetic cell capable of responding to environmental stimuli and subsequently synthesizing proteins responsible for cell mechanical robustness, specifically the production of the *E. coli* cytoskeleton protein MreB. The synthesis of GFP or MreB is controlled by the lac repressor and a Lac01/σ28 amplifier, creating an AND gate consisting of the IPTG inducer and the hypo-osmotic conditions. We further show that when MreB is expressed, it readily associates with the inner membrane of the liposomes, forming a cortex-like structure.

Our overall experimental design is to encapsulate, in phospholipid vesicles, TXTL reactions expressing MscL and couple its mechanosensitivity in response to hypo-osmotic conditions to the influx of chemical inducers which, in turn,

Received: May 5, 2019
Published: July 16, 2019

DOI: 10.1021/acssynbio.9b00204
ACS Synth. Biol. 2019, 8, 1913−1920

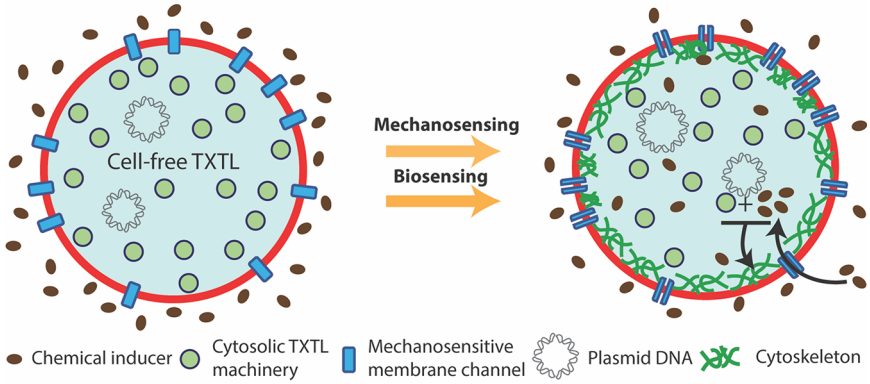

Figure 1. Schematic depicting the proposed synthetic cell's transition from its native state to an active state (development of cell-like cytoskeletal cortex) in response to mechanical and chemical stimuli.

change the phenotype of synthetic cells (Figure 1). The TXTL system supplies both a cytosolic environment and the machinery to express proteins from plasmid DNA. While we made a mechanosensitive vesicle in our previous study,[17] in this work, we explored ways to couple mechanosensitivity with gene expression. The interior of the liposome contains a TXTL reaction and plasmid DNA, while the exterior feeding solution contains a chemical inducer that regulates gene expression by either binding mRNA or sequestering a repressor. When this liposome is in an iso-osmotic environment, the inducer cannot cross the bilayer membrane. However, upon hypo-osmotic conditions, the channels open and the membrane becomes permeable to the inducer. Subsequently, the *E. coli* cytoskeleton protein MreB is expressed and associates with the inner membrane of the liposome. Such synthetic cell system has not been achieved previously because it requires engineering and coordinating several processes in micron-sized compartments. First, tight and inducible genetic regulation has to be achieved in liposomes. Second, the bilayer has to be functionalized with stress-responsive membrane proteins to enable selective and adaptive permeability. Third, the output of the circuit has to be specific to the applied stress. In our pursuit of this goal, we designed and tested three synthetic cell prototypes. We describe our motivations for each iteration. All the DNA circuits were first tested in batch mode TXTL reactions to optimize and characterize plasmid stoichiometry before encapsulation in cell-sized liposomes.

RESULTS AND DISCUSSION

Toehold switches are a class of synthetic riboregulators that have been developed to have both a high degree of orthogonality and a high dynamic range.[20] They typically function using the secondary structures available to mRNA, with the ribosome binding site (RBS) and start codon masked in an RNA hairpin. Upstream of this hairpin is a "switch" sequence, which can be bound by a "trigger" transcript. When bound by the trigger, the hairpin unfolds and the RBS becomes available for translation initiation. These switches can be engineered to work with arbitrary sequences, allowing for the creation of a large set of toehold switches in a potential synthetic cell.[21] Given their versatility and ability to be used as regulators in simultaneous translation of orthogonally expressed proteins, we aimed to implement toehold switches in our first generation of mechanosensitive, genetically adaptive synthetic cell prototype. Using the strong T7 promoter, we cloned toehold switch and trigger sequences previously tested[20] into separate plasmids, T7p14-switch-deGFP, which uses the switch to control the expression of deGFP, and T7p14-trigger, which expresses the 30-nucleotide trigger sequence corresponding to the specific switch. In bulk TXTL reactions (2 μL) expressing T7 RNAP from the P70a-T7RNAP plasmid, this switch gave an ON/OFF ratio of 75−80 while expressing 5−6 μM active deGFP protein (Figure S1a). To improve the ON/OFF ratio and to increase protein expression, we designed an amplified toehold switch using sigma factor 28 (σ28) from *E. coli*. The promoter corresponding to σ28, P28a, has a high affinity for the *E. coli* RNAP/σ28 holoenzyme characterized by a high protein expression with relatively low levels of σ28 as only 1−2 μM σ28 is needed for optimal expression. Using such a strong sigma factor also minimizes the load on the system such that other proteins can be produced. Instead of using the trigger sequence to allow translation of deGFP, we placed σ28 under the control of the switch using a P70a-switch-σ28 plasmid and expressed deGFP using the P28a-deGFP plasmid.[19] In doing this, we do not waste TXTL resources expressing large quantities of switch-σ28 mRNA, since only a small amount is needed to drive expression *via* P28a. The trigger RNA was still produced using a T7 cascade. With this scheme, the ON/OFF ratio increased over 2-fold, up to a ratio of 176, while deGFP expression increased by a factor of 6 to 39 μM (Figure S1b).

Our next step was to demonstrate that this amplified toehold switch functioned without expressing the trigger RNA from a plasmid, but by adding to the reaction an oligonucleotide that could be used as an inducer. Testing the amplifier with ssDNA in batch mode TXTL reactions, we searched for a stoichiometric regime where we could observe a strong and specific induction. We found the optimal concentrations to be 50 μM trigger ssDNA and 1 nM P70a-switch-σ28 plasmid (Figure 2a). Using 5 nM P28a-deGFP plasmid along with the aforementioned concentrations of trigger ssDNA and P70a-switch-σ28, we expressed 31 μM deGFP while maintaining an ON/OFF ratio of 140. Although protein expression increased when the concentration of P70a-switch-σ28 was set to 4 nM, control over the amplified toehold dramatically decreased, with the circuit active even in the absence of trigger ssDNA. This leak resulting in the production of σ28, though small, is enough to drive moderate TXTL expression through the P28a promoter.

On the basis of our findings from batch mode toehold reactions, we proceeded to engineer our first synthetic cell prototype by encapsulating TXTL reactions in double

DOI: 10.1021/acssynbio.9b00204
ACS Synth. Biol. 2019, 8, 1913−1920

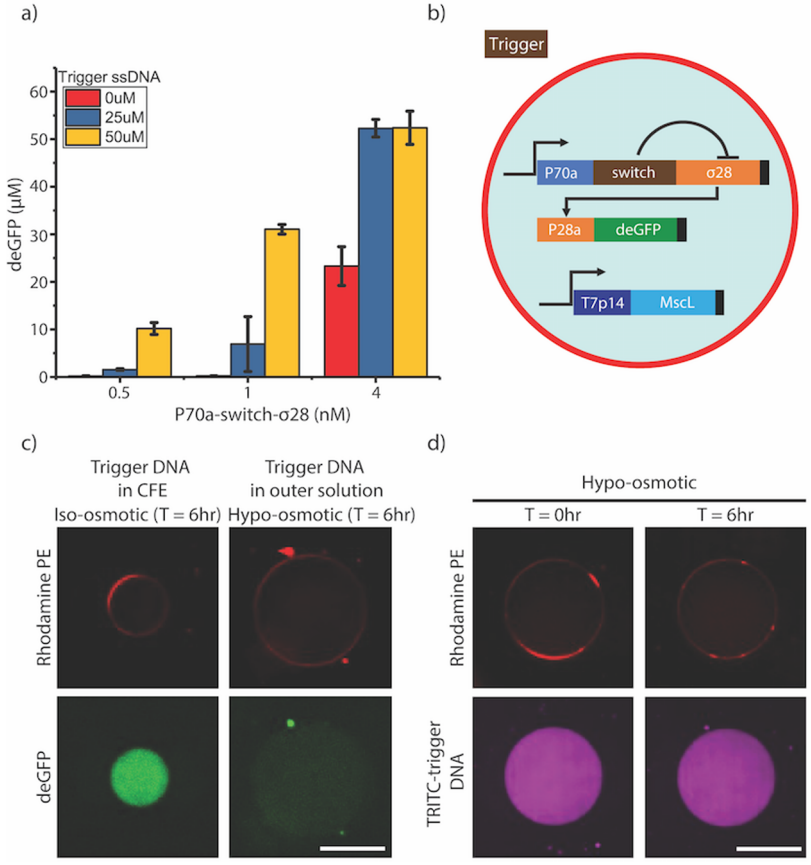

Figure 2. (a) Plot showing the end point deGFP expression of the toehold switch cascade with different concentrations of switch plasmid and the trigger ssDNA in TXTL reactions performed in batch mode reactions. (b) Schematic representing the first minimal cell model where the toehold switch cascade is encapsulated along with a TXTL reaction inside liposomes, orthogonally programmed to express MscL through the T7 promoter, which are then exposed to an outer solution containing the trigger ssDNA. (c) Images of liposomes expressing deGFP with the trigger ssDNA inside (iso-osmotic conditions) or outside (hypo-osmotic conditions) the liposomes, respectively. (d) Images of liposomes expressing MscL containing 50 μM TRITC-labeled trigger ssDNA that are exposed to a hypo-osmotic solution for 6 h. Rhodamine labeled PE lipids were used to visualize liposomal membranes. Scale bar: 50 μm.

emulsion templated cell-sized phospholipid bilayer vesicles. The TXTL reactions contained an amplified toehold switch with its activation dependent on the influx of trigger ssDNA through MscL generated by a T7 cascade (Figure 2b). As a positive control, the trigger ssDNA was encapsulated inside the vesicles under iso-osmotic conditions and compared with adding the trigger sequence to the exterior solution under hypo-osmotic conditions. The reaction output was measured by the fluorescence of deGFP in the lumen of the vesicles. After 6 h, the reactions with the trigger ssDNA inside produced 9−10 times more deGFP than those with the trigger in the external solution under hypo-osmotic condition (Figure 2c, S2a). This suggests that the trigger ssDNA might not be able to enter the vesicles through MscL under hypo-osmotic conditions. To confirm this, fluorescently labeled trigger ssDNA was encapsulated and the leakage through MscL was monitored under hypo-osmotic conditions (Figure 2d). No statistically significant change in the fluorescence intensities after 6 h was observed, confirming that the 30-nt trigger ssDNA is too large to pass through the ∼2.5 nm diameter pore[22] (Figure S2b). Given the ionic strength of the buffer in which the liposomes were incubated in, we assumed the persistence length of ssDNA to be between 2−5 nm.[23,24] This suggests that the trigger sequence could potentially pass through the pore in hypo-osmotic conditions without considering reptation, which would require much longer time scales.

The second synthetic cell prototype was based upon one of the most studied genetic signaling pathways in bacteria: the *lac* operon. Generally, this pathway regulates *E. coli*'s ability to consume lactose in the absence of glucose. We used the synthetic regulatory part, PL-LacO1, consisting of a strong σ70 promoter and two lac operators.[25] The *lac* repressor gene *lacI* and the reporter gene *degfp* were cloned under the synthetic promoters PL-TetO1 and PL-LacO1, respectively; synthesis of MscL remained under the control of the T7 promoter. TXTL reactions containing these plasmids were encapsulated inside liposomes while IPTG, which inhibits repression by LacI, was added to the external feeding solution (Figure 3a).

Initially, no deGFP fluorescence was observed inside the vesicles. After 6 h, there was a 5-fold increase in fluorescence intensities of vesicles exposed to hypo-osmotic conditions, while an increase of less than a factor of 2 was observed in vesicles kept at iso-osmotic conditions (Figure 3b). These data suggest that gene expression is induced by IPTG entering the vesicles through MscL and this predominantly occurs in response to osmotic pressure differences between the internal and external solutions. In the absence of MscL and in hypo-osmotic conditions, a slight induction close to background level was observed when IPTG was added in the external

DOI: 10.1021/acssynbio.9b00204
ACS Synth. Biol. 2019, 8, 1913−1920

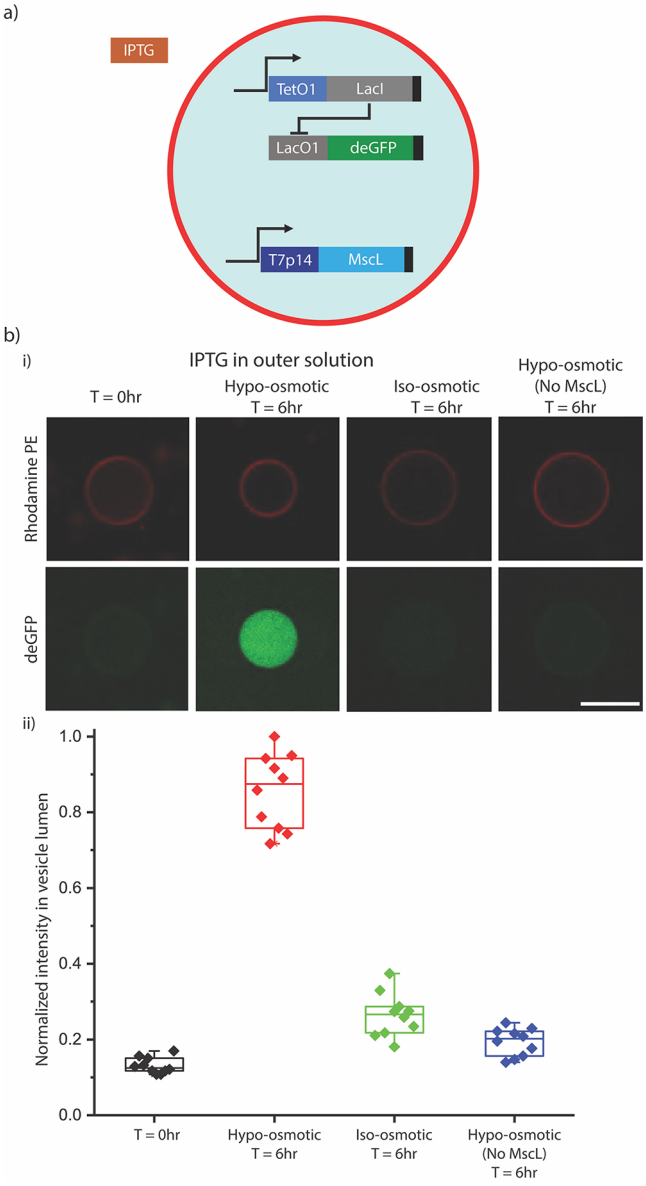

Figure 3. (a) Schematic depicting the second model of the proposed synthetic cell coexpressing an inducible gene circuit and MscL constitutively. IPTG, the inducer, is in the outer solution. (b) (i) Fluorescence images showing expression of deGFP inside liposomes exposed to outer solutions with IPTG and different osmotic conditions at 0 and 6 h. (ii) Box plot of deGFP fluorescence in the vesicle lumen under the different osmotic conditions. Ten liposomes were measured for each condition. Rhodamine labeled PE lipids were used to visualize liposomal membranes. Boxes indicate 20th and 80th percentile values for each condition. Scale bar: 50 μm.

solution (Figure 3b). In the absence of IPTG, a slight leak of the PL-LacO1 induction system was observed (Figure S3). Both tests suggest that the leak observed in the iso-osmotic condition (Figure 3b(ii)) is primarily due to the construct design and not due to the small amount of IPTG influx under iso-osmotic conditions.

The PL-LacO1 promoter offers strong gene repression but is too weak in TXTL. As is, however, the magnitude of the circuit output is too weak to induce the expression of MreB at a concentration sufficiently high to assemble at the inner membrane of liposomes because the critical concentration for polymerization of MreB is estimated to be around 1.5 μM[26] (Figure 4a). To overcome this problem, we developed an amplifier, again using the σ28 cascade.

The *σ28* gene was cloned under the PL-Lac01 promoter and *degfp* was placed under the control of the P28a promoter. LacI now repressed the production of σ28, without which deGFP could not be expressed. The standard PL-Lac01 promoter showed linear protein expression in bulk reactions 30 min after the beginning of the reaction when 200 μM IPTG was added from the start (Figure 4a,b). The case where the reaction was allowed to incubate for 1 h before the addition of IPTG was also tested to ensure that the circuit can indeed be induced when LacI is already blocking the promoter site. This was important to simulate delayed induction of the proposed synthetic cells post assembly due to an externally triggered osmotic shock. When this was done, protein expression was identical to a reaction without IPTG for 90 min, when deGFP fluorescence could be measured. Once protein expression began, the synthesis rates in both cases were the same, around 0.1 μM/h. In the amplified PL-Lac01 circuit with IPTG present from the start, there was a greater delay (60 min as opposed to 30 min) between the onset of the reaction and the measurement of deGFP fluorescence as σ28 needs to be expressed prior to deGFP. The delay in reactions induced after 60 min was likewise longer than in the unamplified circuit, with protein production not evident until 60 min from induction. Again, the rates of protein expression were the same in this linear regime, around 5 μM/h (Figure 4c,d). After both circuits were incubated until completion (>12 h), the amplified circuit produced 38.5 μM deGFP compared to 1.3 μM for the unamplified circuit. The amplified inducible circuit also gave a large ON/OFF ratio (presence *vs* absence of 200 μM IPTG) of 298 compared to 11 for the unamplified circuit, making it ideal for the purposes of this work (Figure 4e).

We have shown thus far that gene expression can be regulated *via* mechanosensing and biosensing. Given the overarching goal of designing a functional minimal cell, we aimed to advance beyond expressing a reporter protein in the third prototype of synthetic cells. A fluorescent MreB fusion protein (Venus-MreB) was placed under the control of P28a which, in turn, was placed under the control of PL-LacO1. Thus, Venus-MreB would only be expressed in the presence of IPTG (Figure 5a).

After 6 h of incubation under hypo-osmotic conditions, vesicles containing the T7p14-MscL plasmid showed fluorescence at the lipid bilayer while those not expressing MscL did not (Figure 5b). The positive control, in which IPTG was encapsulated along with the TXTL reaction in iso-osmotic conditions, showed the same localization of MreB at the membrane, confirming that the observation made in hypo-osmotic conditions with IPTG outside was caused by the influx of inducer through the transiently opened MscL. The concentration of fluorescence at the membrane suggests that MreB is associated with the inner membrane and forms a strikingly different fluorescence pattern than that of deGFP only (Figure 5c). MreB is known to localize at phospholipid bilayers when expressed *in vitro*.[27,28] In hypo-osmotic condition, we did not observe polymerization of MreB in the case without MscL as any leaky expression is likely below the critical concentration for MreB to polymerize. In contrast, in MscL-expressing vesicles, the formation of a ring-like structure was prominent in ~90% of the liposomes exposed to the hypo-osmotic shock post synthesis. While the intensities varied owing to different levels of induction and IPTG influx, they

DOI: 10.1021/acssynbio.9b00204
ACS Synth. Biol. 2019, 8, 1913−1920

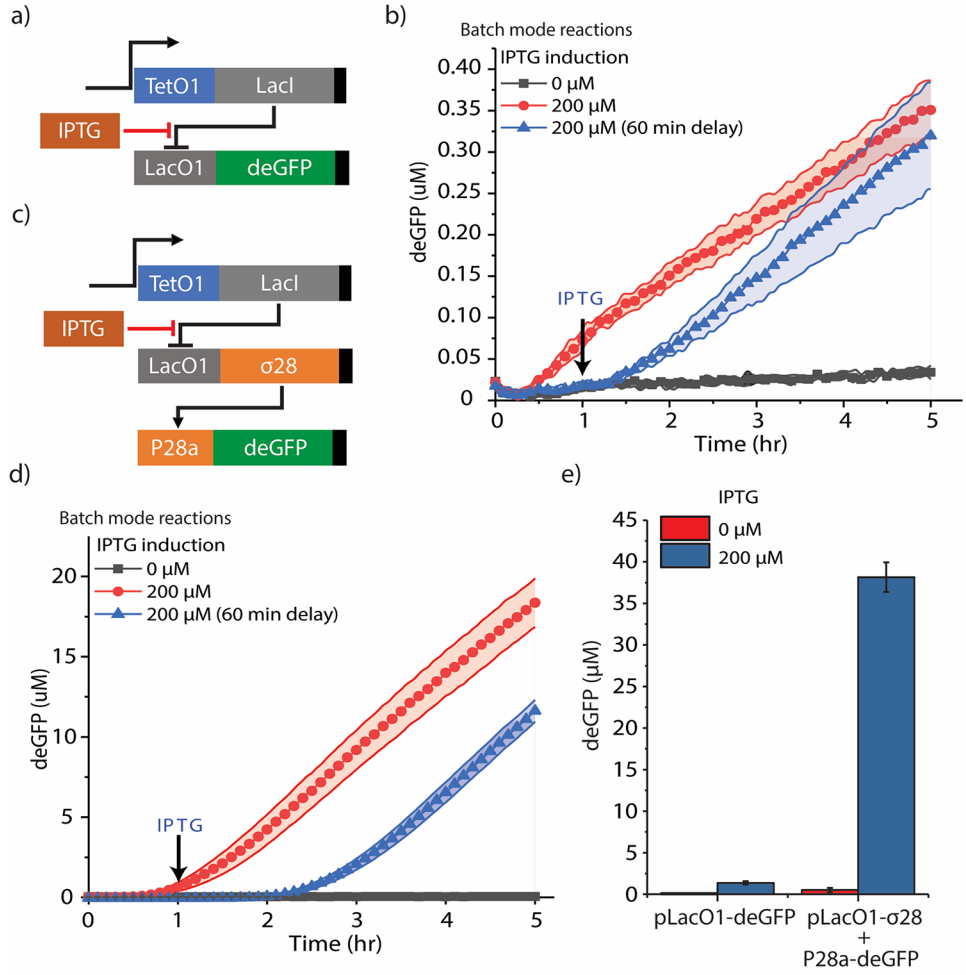

Figure 4. (a) Schematic of the unamplified inducible gene circuit. (b) Kinetics of deGFP expression in batch mode TXTL reactions using the circuit shown in (a) with no IPTG; induction at time T = 0 h; and delayed induction at time T = 1 h. (c) Schematic of an amplified inducible circuit using the σ28 cascade. (d) Kinetics of deGFP expression in batch mode TXTL reactions using the circuit shown in (c) with no IPTG; induction at time T = 0 h; and delayed induction at time T = 1 h. (e) Plot of end point deGFP expression with and without IPTG induction after 14 h for the gene circuits shown in (a) and (c).

were always slightly lower than the control scenario with IPTG encapsulated inside liposomes which can be attributed to delayed influx of IPTG though MscL and depletion of resources while incubating in iso-osmotic conditions prior to the hypo-osmotic shock. No physical deformation of the membrane was observed supposedly because the tension at the membrane is too high. Nevertheless, the assembly of a cortex-like MreB structure would presumably provide the vesicles with stronger mechanical resistance to external mechanical stresses, similar to the effect of what an actin cortex has in a mammalian cell.[29]

CONCLUSIONS

While generating a synthetic cell model capable of expressing multiple proteins with temporal and spatial variation is desirable to better understand and mimic cellular processes, it is important to reconstitute intercellular and extracellular interactions toward enabling the synthetic cells to respond to external, time-varying stimuli. The synthetic cell developed here is one such example and can be expanded further by leveraging orthogonal TXTL reactions to mediate simultaneous or sequential induction with different membrane impermeable molecules, thus providing modularity in the number of different systems that can be reconstituted within the same compartment. Prior to this work, liposomes were programmed with DNA to execute inducible gene circuits,[8,30,31] to express cytoskeleton proteins from *E. coli*[28] and, in separate experiments by these authors, to generate mechanosensitive biosensors.[17] To our knowledge, this is the first work that couples an external stimulus to inducible gene expression by way of mechanosensitivity. Our experiments provide information, including positive and negative results, on how to integrate multiple biological mechanisms into a synthetic cell system involving membrane properties and inducible gene expression. The experimental approach presented in this work could be used to learn the dynamics of multiprotein interactions or step-by-step assembly in order to better understand the complexities of real cells.

METHODS

Materials. All reagents unless otherwise mentioned were purchased from Sigma-Aldrich (St. Louis, MO). Lipids were purchased from Avanti Polar Lipids Inc. (Alabaster, AL). Synthetic DNA was purchased from Integrated DNA Technologies (Coralville, IA).

DOI: 10.1021/acssynbio.9b00204
ACS Synth. Biol. 2019, 8, 1913−1920

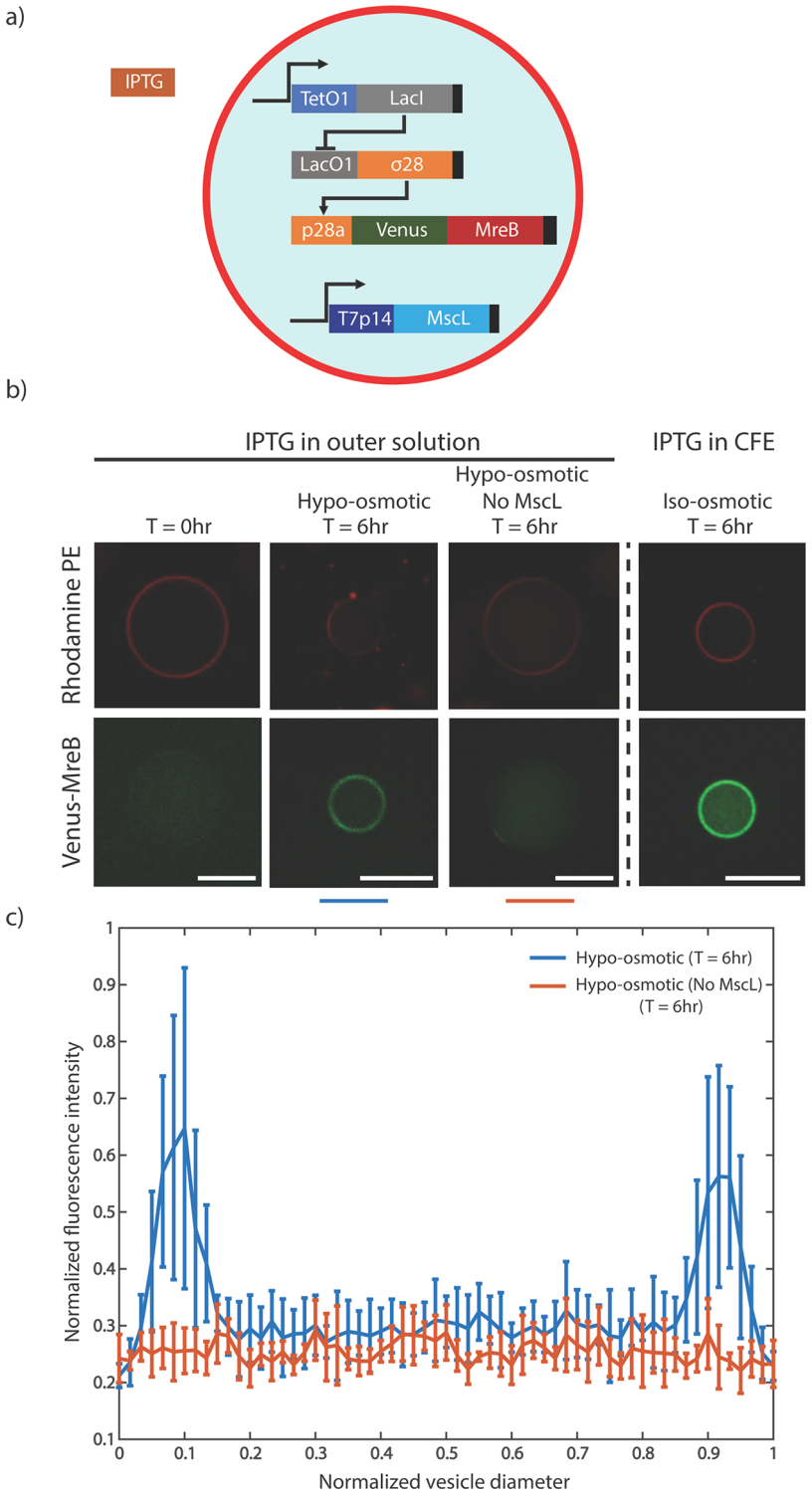

Figure 5. (a) Schematic depicting the third proposed synthetic cell system coexpressing an amplified gene circuit encoding the gene for Venus-MreB and MscL constitutively. The liposomes were placed in a feeding solution containing 200 μM IPTG, except for the control experiment (IPTG inside liposomes). (b) IPTG induction of synthetic cells in outer solutions containing IPTG and different osmotic conditions over a time duration of 6 h and a positive control experiment with IPTG inside the liposomes. (c) Line scans of liposomes normalized with respect to their diameters and the maximum intensity among all liposomes observed. Five liposomes for each condition reported were analyzed. Error bars indicate standard deviation of the normalized data. Rhodamine labeled PE lipids were used to visualize liposomal membranes. Scale bars: 50 μm.

DNA Constructs. The plasmids P70a-σ28, P28a-deGFP, P70a-T7RNAP, and T7p14-deGFP have been described previously.[19] P28a-Venus-MreB was obtained by inserting Venus-MreB[28] into a P28a backbone between *Sal*I and *Bam*HI. T7p14-MscL was obtained by cloning MscL into a backbone. Specifically, MscL was obtained *via* PCR from *E. coli* K12 and inserted into a T7p14 backbone between restriction sites XbaI and XhoI. The switch/trigger pair used was first described by Green *et al.* as toehold switch number 10 in their set of forward-engineered toehold switches in Table S3.[20] The

DOI: 10.1021/acssynbio.9b00204
ACS Synth. Biol. 2019, 8, 1913−1920

plasmid P70a-switch-σ28 was constructed by inserting a gBlock gene fragment (IDT) into the plasmid P70a-σ28 between NheI and *Bam*HI. The plasmid T7p14-trigger was cloned by inserting a gBlock gene fragment (IDT) of the trigger sequence into T7p14-deGFP between *Bgl*II and XhoI. T7p14-switch-deGFP was obtained by inserting a gBlock gene fragment (IDT) of the switch-deGFP sequence into T7p14-deGFP between XbaI and XhoI. The single stranded trigger DNA (ssDNA) fragment was ordered from IDT and resuspended in water at 500 μM. The LacO1 and TetO1 plasmids were constructed using synthetic regulatory parts.[25]

TXTL Reactions. The myTXTL kit (Arbor Biosciences) was used. TXTL reactions are composed of an *E. coli* lysate, an amino acid mixture, an energy buffer, and the desired DNA templates. The preparation of the lysate used for TXTL has been extensively described in prior works.[32,19] The lysate represents roughly one-third of the total reaction volume and contains the endogenous machinery required for both transcription and translation. The amino acid mixture is an equimolar blend of the 20 canonical amino acids, with the total amino acid concentration in the final reaction fixed between 2 and 4 mM. When linear DNA was used, Chi6 was added to the reaction at 2 μM to prevent degradation.[33]

Bulk Expression Assay. Fluorescence from batch mode TXTL reactions was measured using the reporter protein deGFP (25.4 kDa, 1 mg/mL = 39.4 μM), a more translatable version of GFP in TXTL.[34] Fluorescence was measured at 3 min intervals using monochromators (Ex/Em 488/525 nm) on Biotek Syngery H1 plate readers in Nunc polypropylene 96-well, V-bottom plates. End point reactions were measured after 8−12 h of incubation. To measure protein concentration, a linear calibration curve of fluorescence intensity *versus* eGFP concentration was generated using purified recombinant eGFP obtained from Cell Biolabs, Inc. or purified in the lab. All reactions were incubated at 29 °C in either a benchtop incubator, for end-point measurements, or in the plate readers, for kinetic measurements.

Liposome preparation. Liposomes were prepared using a microfluidic device suitable for encapsulating complex biochemical solutions as illustrated in detail in a previous publication.[12] Briefly, W/O/W double emulsions were made using the cell-free solution as the inner phase and a buffer solution (20 mM K-HEPES pH 7.5, 70 mM potassium chloride, 1.3% glycerol, 10% poly(vinyl alcohol), 1% Pluronic F-68, 10 mM magnesium chloride and 170 mM glucose) as the outer aqueous phase. A mixture of DOPC, DOPE, cholesterol and Liss-Rhod PE in the ratio of 60:9.9:30:0.1 by mole was prepared in a glass vial which was then subjected to a steady stream of argon gas to remove residual chloroform from the mixture and generate a pseudo dry lipid film on the glass surface. The glass vial was then placed under vacuum for 2 h at room temperature to ensure minimal traces of residual chloroform before resuspending in 1 mL of oil phase (hexane and chloroform in a ratio of 64:36 by volume). 750 μL of formed double emulsion solution was collected in an epi tube and incubated at 29 °C for 1 h following which 250 μL of buffer containing 20 mM K-HEPES pH 7.5, 10% PVA and 10 mM IPTG or 100 μM trigger DNA was added to get a final outer solution with osmolality ∼100 mOsm/kg less than the inner cell-free solution. This osmotic difference was chosen as we had previously observed the activity of MscL at such a difference. The osmolarities were measured prior to liposome encapsulation using a vapor pressure osmometer (Vapro, Wescor). The osmolality of the cell-free reaction was previously measured to increase with time by about 1.5−2% depending on the type of protein being expressed. Following the incubation for 1 h and subsequent addition of buffer containing IPTG or trigger DNA, the now formed liposomes were gently filled into imaging chambers on a glass slide, sealed and allowed to incubate at 29 °C for 6 h.

Imaging. All images of liposomes were taken with an inverted spinning disk confocal microscope setup. An Olympus IX-81 scope connected to an Andor iXon3 CCD camera were used to image the liposomes. Solid state lasers with ALC tuning (488 nm for deGFP and 561 nm for Liss-Rhod PE) were used to excite the liposomes, respectively. All image analysis was carried out in ImageJ. In order to quantify fluorescence intensities when using the fluorescent trigger or following IPTG induction of deGFP synthesis, three large rectangular regions of interest were randomly made inside the lumen of each liposome and the average intensity calculated. Thereafter the same three regions were translated to the outside of the liposomes to record the average background intensities. The final background corrected intensities as calculated were normalized and plotted in Origin Pro. For the line scan plot, three lines of equal length were drawn across a single liposome and the average values of the intensities were calculated after background subtraction. The intensity values for the liposome corresponding to the positive control scenario was normalized with respect to its maximum value while the other two liposome intensities were normalized by dividing by the maximum value of the liposome under hypo-osmotic condition subjected to IPTG induction. In order to normalize the line plot intensities with respect to the diameter of each liposome, the smallest liposome diameter was chosen as the reference line. The intensities for all the liposomes were then parsed into the total number of data points available for this reference liposome. A MATLAB code was written to carry out the above procedure. The plots for the Supplementary Figures were generated in Origin Pro. All error bars indicate the standard deviation of all data collected for each condition.

■ ASSOCIATED CONTENT

Supporting Information

The Supporting Information is available free of charge on the ACS Publications website at DOI: 10.1021/acssynbio.9b00204.

Supplementary data, Figures S1−S3 (PDF)

■ AUTHOR INFORMATION

Corresponding Authors

*E-mail: allenliu@umich.edu.
*E-mail: noireaux@umn.edu.

ORCID

Allen P. Liu: 0000-0002-0309-7018
Vincent Noireaux: 0000-0002-5213-273X

Author Contributions

#J.G. and S.M. contributed equally. J.G. and S.M. performed the experiments, J.G., S.M., A.P.L., and V.N. analyzed the data and wrote the manuscript.

Notes

The authors declare the following competing financial interest(s): The Noireaux laboratory receives research funds

DOI: 10.1021/acssynbio.9b00204
ACS Synth. Biol. 2019, 8, 1913−1920

from Arbor Biosciences, a distributor of the myTXTL cell-free protein synthesis kit.

■ ACKNOWLEDGMENTS

This work is supported by the National Science Foundation MCB-1612917 to A.P.L. and MCB-1613677 to V.N., and the Human Frontier Science Program grant number RGP0037/2015 to V.N.

■ REFERENCES

(1) Majumder, S., and Liu, A. P. (2018) Bottom-up Synthetic Biology: Modular Design for Making Artificial Platelets. *Phys. Biol. 15*, 013001.
(2) Caschera, F., and Noireaux, V. (2014) Integration of Biological Parts toward the Synthesis of a Minimal Cell. *Curr. Opin. Chem. Biol. 22*, 85.
(3) Chiarabelli, C., Stano, P., and Luisi, P. L. (2009) Chemical Approaches to Synthetic Biology. *Curr. Opin. Biotechnol. 20* (4), 492−497.
(4) Hutchison, C. A., Chuang, R. Y., Noskov, V. N., Assad-Garcia, N., Deerinck, T. J., Ellisman, M. H., Gill, J., Kannan, K., Karas, B. J., Ma, L., et al. (2016) Design and Synthesis of a Minimal Bacterial Genome. *Science (Washington, DC, U. S.) 351*, aad6253.
(5) Schwille, P. (2015) Jump-Starting Life? Fundamental Aspects of Synthetic Biology. *J. Cell Biol. 210*, 687.
(6) Ishikawa, K., Sato, K., Shima, Y., Urabe, I., and Yomo, T. (2004) Expression of a Cascading Genetic Network within Liposomes. *FEBS Lett. 576* (3), 387−390.
(7) Noireaux, V., and Libchaber, A. (2004) A Vesicle Bioreactor as a Step toward an Artificial Cell Assembly. *Proc. Natl. Acad. Sci. U. S. A. 101* (51), 17669.
(8) Caschera, F., and Noireaux, V. (2016) Compartmentalization of an All-*E. coli* Cell-Free Expression System for the Construction of a Minimal Cell. *Artif. Life 22* (2), 185.
(9) Liu, A. P., and Fletcher, D. A. (2009) Biology under Construction: In Vitro Reconstitution of Cellular Function. *Nat. Rev. Mol. Cell Biol. 10*, 644.
(10) Lu, Y. (2017) Cell-Free Synthetic Biology: Engineering in an Open World. *Synth. Syst. Biotechnol. 2*, 23.
(11) Garamella, J., Garenne, D., and Noireaux, V. (2019) TXTL-Based Approach to Synthetic Cells. *Methods Enzymol. 617*, 217.
(12) Ho, K. K. Y., Murray, V. L., and Liu, A. P. (2015) Engineering Artificial Cells by Combining HeLa-Based Cell-Free Expression and Ultrathin Double Emulsion Template. *Methods Cell Biol. 128*, 303.
(13) Lentini, R., Martín, N. Y., Forlin, M., Belmonte, L., Fontana, J., Cornella, M., Martini, L., Tamburini, S., Bentley, W. E., Jousson, O., et al. (2017) Two-Way Chemical Communication between Artificial and Natural Cells. *ACS Cent. Sci. 3*, 117.
(14) Deng, N. N., Yelleswarapu, M., and Huck, W. T. S. (2016) Monodisperse Uni- and Multicompartment Liposomes. *J. Am. Chem. Soc. 138*, 7584.
(15) Vogele, K., Frank, T., Gasser, L., Goetzfried, M. A., Hackl, M. W., Sieber, S. A., Simmel, F. C., and Pirzer, T. (2018) Towards Synthetic Cells Using Peptide-Based Reaction Compartments. *Nat. Commun.*, DOI: 10.1038/s41467-018-06379-8.
(16) Noireaux, V., and Libchaber, A. (2004) A Vesicle Bioreactor as a Step toward an Artificial Cell Assembly. *Proc. Natl. Acad. Sci. U. S. A. 101* (51), 17669−17674.
(17) Majumder, S., Garamella, J., Wang, Y.-L., Denies, M., Noireaux, V., and Liu, A. P. (2017) Cell-Sized Mechanosensitive and Biosensing Compartment Programmed with DNA. *Chem. Commun. 53* (53), 7349.
(18) Garenne, D., and Noireaux, V. (2019) Cell-Free Transcription−Translation: Engineering Biology from the Nanometer to the Millimeter Scale. *Curr. Opin. Biotechnol. 58*, 19.
(19) Garamella, J., Marshall, R., Rustad, M., and Noireaux, V. (2016) The All *E. coli* TX-TL Toolbox 2.0: A Platform for Cell-Free Synthetic Biology. *ACS Synth. Biol. 5* (4), 344.
(20) Green, A. A., Silver, P. A., Collins, J. J., and Yin, P. (2014) Toehold Switches: De-Novo-Designed Regulators of Gene Expression. *Cell 159*, 925.
(21) Pardee, K., Green, A. A., Takahashi, M. K., Braff, D., Lambert, G., Lee, J. W., Ferrante, T., Ma, D., Donghia, N., Fan, M., et al. (2016) Rapid, Low-Cost Detection of Zika Virus Using Programmable Biomolecular Components. *Cell 165*, 1255.
(22) Martinac, B. (2004) Mechanosensitive Ion Channels: Molecules of Mechanotransduction. *J. Cell Sci. 117*, 2449.
(23) Chen, H., Meisburger, S. P., Pabit, S. A., Sutton, J. L., Webb, W. W., and Pollack, L. (2012) Ionic Strength-Dependent Persistence Lengths of Single-Stranded RNA and DNA. *Proc. Natl. Acad. Sci. U. S. A. 109*, 799.
(24) Rechendorff, K., Witz, G., Adamcik, J., and Dietler, G. (2009) Persistence Length and Scaling Properties of Single-Stranded DNA Adsorbed on Modified Graphite. *J. Chem. Phys. 131*, 095103.
(25) Lutz, R., and Bujard, H. (1997) Independent and Tight Regulation of Transcriptional Units in *Escherichia coli via* the LacR/O, the TetR/O and AraC/I-1-I-2 Regulatory Elements. *Nucleic Acids Res. 25* (6), 1203−1210.
(26) Nurse, P., and Marians, K. J. (2013) Purification and Characterization of *Escherichia coli* MreB Protein. *J. Biol. Chem. 288*, 3469.
(27) Salje, J., van den Ent, F., de Boer, P., and Löwe, J. (2011) Direct Membrane Binding by Bacterial Actin MreB. *Mol. Cell 43*, 478.
(28) Maeda, Y. T., Nakadai, T., Shin, J., Uryu, K., Noireaux, V., and Libchaber, A. (2012) Assembly of MreB Filaments on Liposome Membranes: A Synthetic Biology Approach. *ACS Synth. Biol. 1* (2), 53.
(29) Tinevez, J.-Y., Schulze, U., Salbreux, G., Roensch, J., Joanny, J.-F., and Paluch, E. (2009) Role of Cortical Tension in Bleb Growth. *Proc. Natl. Acad. Sci. U. S. A. 106*, 18581.
(30) Adamala, K. P., Martin-Alarcon, D. A., Guthrie-Honea, K. R., and Boyden, E. S. (2017) Engineering Genetic Circuit Interactions within and between Synthetic Minimal Cells. *Nat. Chem. 9*, 431.
(31) Shin Noireaux, V. (2012) An E. coli Cell-Free Expression Toolbox: Application to Synthetic Gene Circuits and Artificial Cells. *ACS Synth. Biol. 1* (1), 29−41.
(32) Sun, Z. Z., Hayes, C. A., Shin, J., Caschera, F., Murray, R. M., and Noireaux, V. (2013) Protocols for Implementing an *Escherichia coli* Based TX-TL Cell-Free Expression System for Synthetic Biology. *J. Visualized Exp.*, DOI: 10.3791/50762.
(33) Marshall, R., Maxwell, C. S., Collins, S. P., Beisel, C. L., and Noireaux, V. (2017) Short DNA Containing χ Sites Enhances DNA Stability and Gene Expression in *E. coli* Cell-Free Transcription−Translation Systems. *Biotechnol. Bioeng. 114* (9), 2137.
(34) Shin, J., and Noireaux, V. (2010) Efficient Cell-Free Expression with the Endogenous *E. coli* RNA Polymerase and Sigma Factor 70. *J. Biol. Eng. 4*, 8.

DOI: 10.1021/acssynbio.9b00204
ACS Synth. Biol. 2019, 8, 1913−1920

Supporting Information

An adaptive synthetic cell based on mechanosensing, biosensing, and inducible gene circuits

Jonathan Garamella[1,+], Sagardip Majumder[2,+], Allen P. Liu[2,3,4,5,*], and Vincent Noireaux[1,*]

[1]Department of Physics and Astronomy, University of Minnesota, Minneapolis, MN 55455
[2]Department of Mechanical Engineering, University of Michigan, Ann Arbor, MI, 48109
[3]Department of Biomedical Engineering, University of Michigan, Ann Arbor, MI, 48109
[4]Cellular and Molecular Biology Program, University of Michigan, Ann Arbor, MI, 48109
[5]Biophysics Program, University of Michigan, Ann Arbor, MI, 48109

[+]Signifies equal contribution
[*]Signifies co-corresponding authors

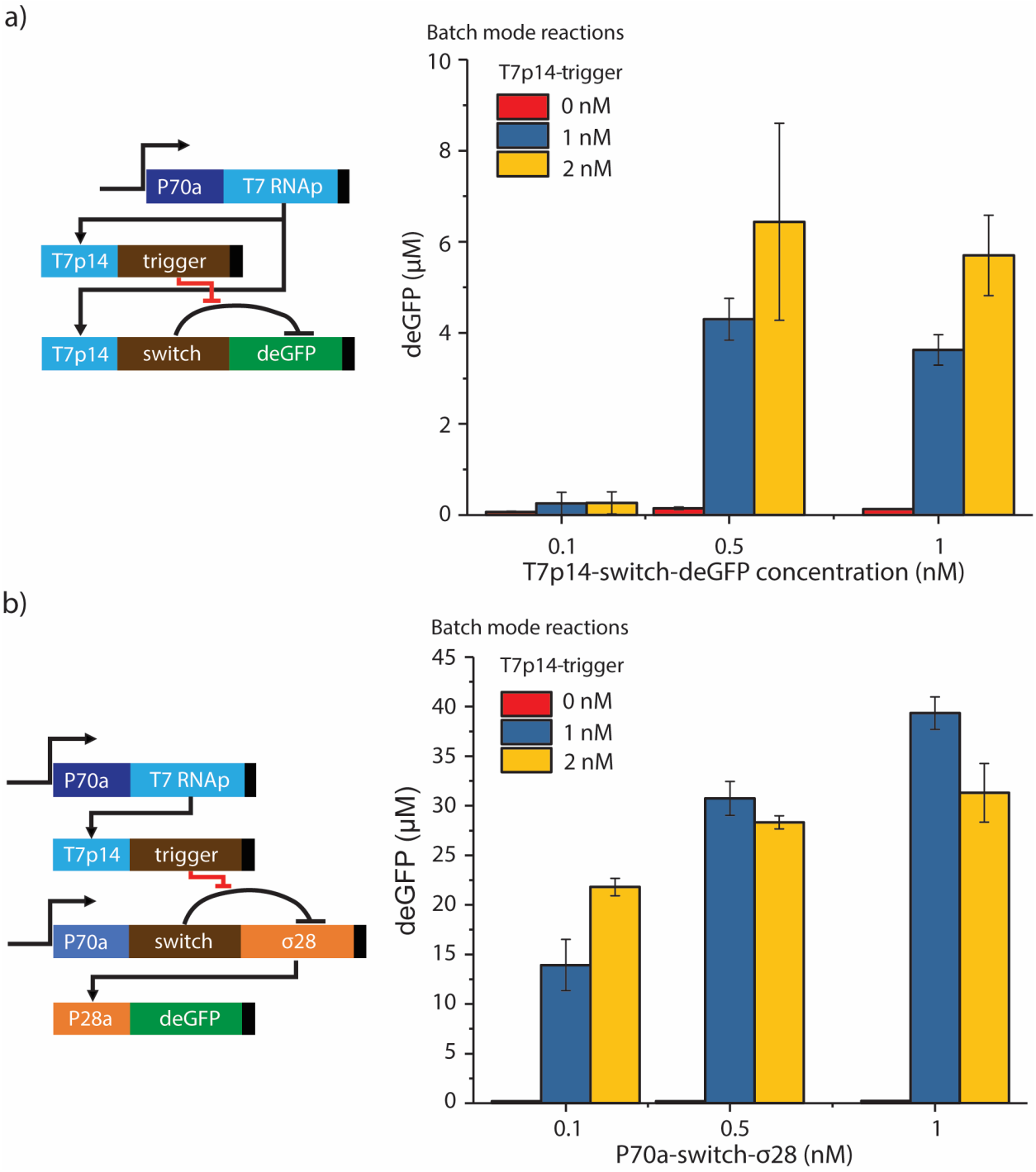

Supplementary Figure 1. a) deGFP expression via the toehold switch cascade using the T7 promotor to express both switch and trigger sequences from plasmid DNA. **b**) deGFP expression via an amplified toehold switch cascade in which the P70a promoter is used to express switch-σ28, and deGFP is expressed via the P28a promoter. Concentrations of switch and trigger plasmids were kept the same as a) and the concentration of P28a-deGFP plasmid was fixed at 5 nM.

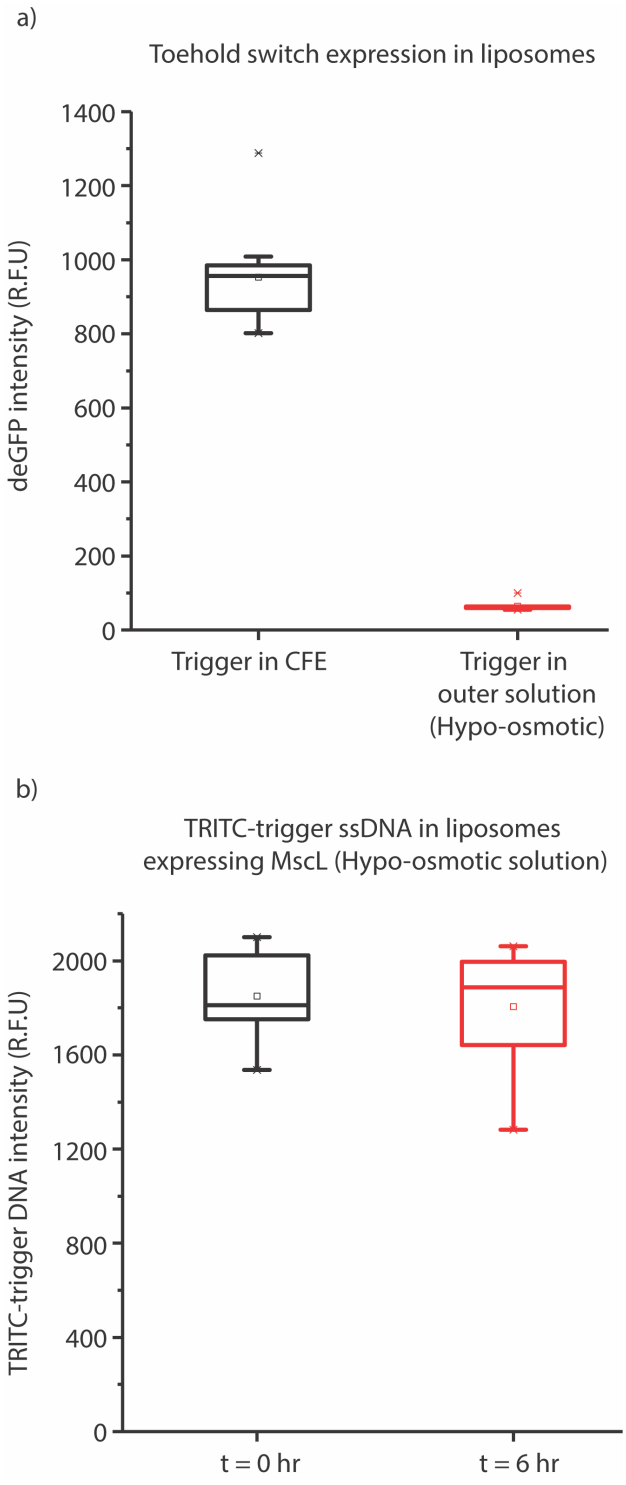

Supplementary Figure 2. a) Boxplot of deGFP fluorescence in the vesicle lumen when 50 μM trigger ssDNA is either inside the vesicle or in the external solution. **b)** Boxplot of TRITC conjugated trigger ssDNA fluorescence in the vesicle lumen at 0 and 6 h after encapsulation and exposure to hypo-osmotic solution. MscL is expressed using the T7 promoter. 10 liposomes observed were analyzed for each condition. Boxes indicate 20th and 80th percentile values for each condition.

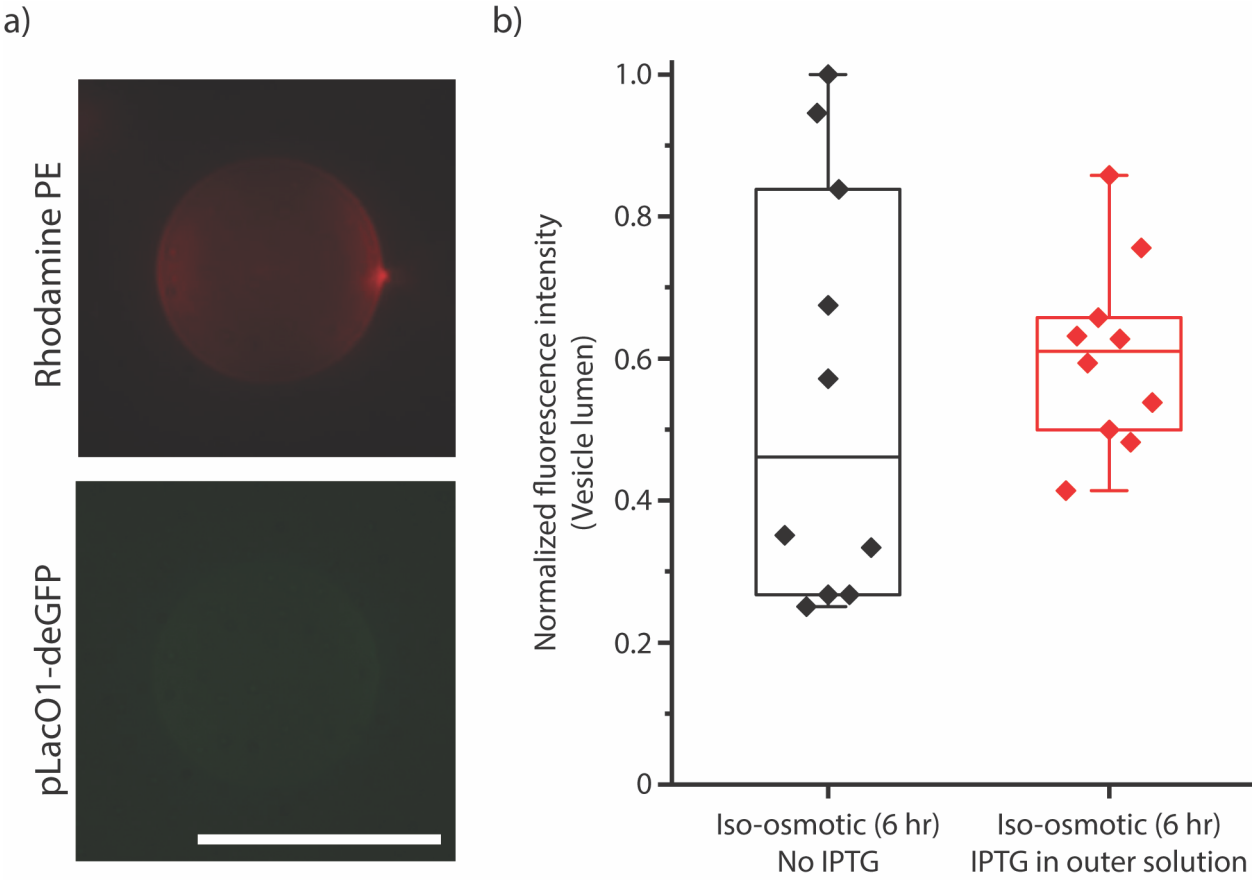

Supplementary Figure 3. a) Images depicting leakiness of the pLacO1-deGFP genetic circuit when expressed in the absence of IPTG in the inner and outer solutions after 6 hours of incubation at 29C. **b)** Box plot comparing the intensity values of vesicle lumen for the condition presented in **a)** with that of the liposomes incubated under isosmotic condition in the presence of IPTG in the outer solution (Fig. 3b(i)). The values were normalized with respect to the maximum intensity value between the two sets of conditions. 10 liposomes observed were analyzed for each condition. Boxes indicate 20^{th} and 80^{th} percentile values for each dataset. Scale bar: 50 μm.